International Journal of Current Engineering and Technology
ISSN 2277 - 4106

Available at http://inpressco.com/category/ijcet

Research Article

A Newly Constructed of Renewable Energy Micro Grid using FUZZY Logic Technique

K.S.Srikanth[Á*] and Indranil Saaki[Ḃ]

[Á]Professor, Department of EEE, KL University, Vijayawada, AP, INDIA.
[Ḃ]Assistant Professor, Department of R&D Global e-Smart Technologies, Visakhapatnam, AP, INDIA.

Accepted 05 November 2013, Available online 01 December 2013, **Vol.3, No.5 (December 2013)**

Abstract

Three Phase ac power systems have existed for over 100 years due to their efficient transformation of ac power at different voltage levels and over long distance as well as the inherent characteristic from fossil energy driven rotating machines. The proposed system presents power-control strategies of a grid-connected Micro grid generation system with versatile power transfer. This Micro grid system allows maximum utilization of freely available renewable energy sources like wind and photovoltaic energies. For this, an adaptive MPPT P&O Controller along with standard perturbs and observes method will be used for the system. In This paper proposes a ac/dc micro grid to reduce the processes of multiple dc–ac–dc or ac–dc–ac conversions in an individual ac or dc grid. The Micro grid consists of both ac and dc networks connected together by multi-bidirectional converters. AC sources and loads are connected to the ac network whereas dc sources and loads are tied to the dc network. Energy storage systems can be connected to dc or ac links. The proposed Micro grid can operate in a grid-tied or autonomous mode. The coordination control algorithms are proposed for smooth power transfer between ac and dc links and for stable system operation under various generation and load conditions. This Micro grid system operates under normal conditions which include normal room temperature in the case of solar energy and normal wind speed at plain area in the case of wind energy. The Power Balancing Control simulation results are presented to illustrate the operating principle, feasibility and reliability of Micro grid proposed system.

Keywords: *Energy management, grid control, grid operation, micro-grid, PV system, wind power generation, Fuzzy logic, UPQC, Power, Fuel cell*

1. Introduction

Increasing electrification of daily life causes growing electricity consumption, rising number of sensitive/critical loads demand for high-quality electricity, the energy efficiency of the grid is desired to be improved, and considerations on climate change are calling for sustainable energy applications (R. H. Lasseter, 2002; Y. Zoka *et al*, 2004). All these factors are driving the conventional electricity grid to the next generation of grid, i.e. smart grid, which is expected to appear and coexist with the existing grid, adding to its capacity, reliability, and functionalities (R. H. Lasseter *et al*, 2004).Consequently, the applications of distributed generation(DG) systems are emerging, and most will be interfaced to the grid through power-electronics converters. However, the grid will become much more complex due to the increasing number of DG systems. For instance, the traditional one way power flow is broken by the bidirectional power flow and the top-down centralized control changes to the bottom up decentralized control. Furthermore, more voltage quality problems may be introduced if the DG systems are not well controlled and organized (C. K. Sao *et al*, 2008). It has been implicated that power electronics-based converters not only can service as interfaces with the utility grid, but also have the potential for mitigating power quality problems (T. Logenthiran *et al* , 2008). Some auxiliary functions such as active filtering have been reported (M. E. Baran *et al*, 2003). Other works such as voltage unbalance compensation, grid support, and ride-through control under voltage dips have been presented in (Y. Ito, 2004; A. Sannino *et al*, 2003). Therefore, to adapt to future smart grid application, it will be a tendency of grid interfacing converters to integrate voltage quality enhancement and DG together. This paper focuses on the grid-interfacing architecture, taking into account how to interconnect DG systems in the future grid with enhanced voltage quality.

An example of the future application of grid-interfacing converters for connecting multiple DG systems to the utility grid.The desirable approach should be able to maintain high-quality power transfer between DG systems

*Corresponding author **K.S.Srikanth** is working as Professor and **Indranil Saaki** as Assistant Professor

and the utility grid, even in disturbed grids, and be able to improve the voltage quality at both user and grid side. Figure 1 shows an example of the future application of grid-interfacing converters. On the left-hand side, multiple DG systems together with energy storage and local loads are interconnected to construct a micro grid. Energy storage systems (e.g., super capacitor, battery, fuel cell, etc. (D. J. Hammerstrom *et al*, 2007)) are used to store excess energy from the micro grid and send the stored energy back to the grid when needed, which are necessary for micro grid applications. As a basic structure of the smart grid, plug-and-play integration of micro grids is essential, which can function whether they are connected to or separate from the electricity grid (D. Salomonsson *et al*, 2007) . On the right-hand side, a bidirectional series converter, which is supplied with distributed source and energy storage, interfaces the micro grid to a utility grid (can be another micro grid) for exchanging power and isolates grid disturbances from each of the grids. The data bus indicates network-scale communication path for variable collection and exchange in smart grid.

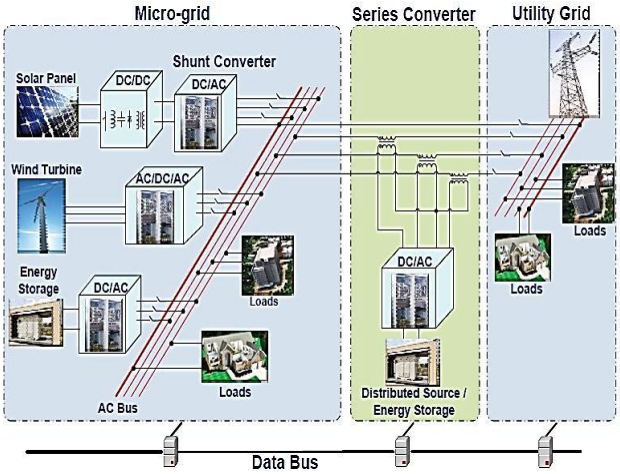

Fig. 1 Future application of grid-interfacing converters

A AC/DC micro grid is proposed in this paper to reduce processes of multiple reverse conversions in an individual ac or dc grid and to facilitate the connection of various renewable ac and dc sources and loads to power system. Since energy management, control, and operation of a Micro Grid are more complicated than those of an individual ac or dc grid, different operating modes of a Micro Grid ac/dc grid have been investigated. The coordination control schemes among various converters have been proposed to harness maximum power from renewable power sources, to minimize power transfer between ac and dc networks, and to maintain the stable operation of both ac and dc grids under variable supply and demand conditions when the Micro Grid operates in both grid-tied and islanding modes. The advanced power electronics and control technologies used in this paper will make a future power grid much smarter. The proposed Micro grid can operate in a grid-tied or autonomous mode. The coordination control algorithms are proposed for smooth power transfer between ac and dc links and for stable system operation under various generation and load conditions. This Micro grid system operates under normal conditions which include normal room temperature in the case of solar energy and normal wind speed at plain area in the case of wind energy. The Power Balancing Control simulation results are presented to illustrate the operating principle, feasibility and reliability of Micro grid proposed system.

2. System Configuration and Modeling

A. Grid Configuration

Fig. 1 shows a conceptual Micro Grid system configuration where various ac and dc sources and loads are connected to the corresponding dc and ac networks. The AC and DC links are connected together through two transformers and two four-quadrant operating three phase converters. The ac bus of the Micro Grid is tied to the utility grid. A compact Micro Grid as shown in Fig. 2 is modeled using the Simulink in the MATLAB to simulate system operations and controls. Forty kW PV arrays are connected to dc bus through a DC/DC boost converter to simulate dc sources. A capacitor C_{ω} is to suppress high frequency ripples of the PV output voltage. A 50 kW wind turbine generator (WTG) with doubly fed induction generator (DFIG) is connected to an ac bus to simulate ac sources. A 65 Ah battery as energy storage is connected to dc bus through a bidirectional DC/DC converter. Variable dc load (20 kW–40 kW) and AC load (20 kW–40 kW) are connected to DC and AC buses respectively. The rated voltages for dc and AC buses are 400 V and 400 V rms respectively. A three phase bi-directional DC/AC main converter with R-L-C filter connects the dc bus to the ac bus through an isolation transformer. A compact representation of the proposed Micro Grid grid.

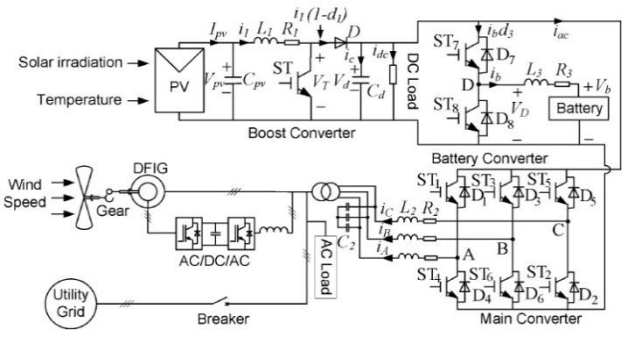

Fig. 2 A compact Micro Grid

B. Grid Operation

The Micro Grid can operate in two modes. In grid-tied mode, the main converter is to provide stable dc bus voltage and required reactive power and to exchange power between the AC and DC buses. The boost converter and WTG are controlled to provide the maximum power. When the output power of the DC sources is greater than the dc loads, the converter acts as an inverter and injects

power from DC to AC side. When the total power generation is less than the total load at the dc side, the converter injects power from the AC to DC side. When the total power generation is greater than the total load in the Micro Grid, it will inject power to the utility grid. Otherwise, the Micro Grid will receive power from the utility grid. In the grid tied mode, the battery converter is not very important in system operation because power is balanced by the utility grid. In autonomous mode, the battery plays a very important role for both power balance and voltage stability. Control objectives for various converters are dispatched by energy management system. DC bus voltage is maintained stable by a battery converter or boost converter according to different operating conditions. The main converter is controlled to provide a stable and high quality ac bus voltage. Both PV and WTG can operate on maximum power point tracking (MPPT) or off-MPPT mode based on system operating requirements. Variable wind speed and solar irradiation are applied to the WTG and PV arrays respectively to simulate variation of power of ac and dc sources and test the MPPT control algorithm.

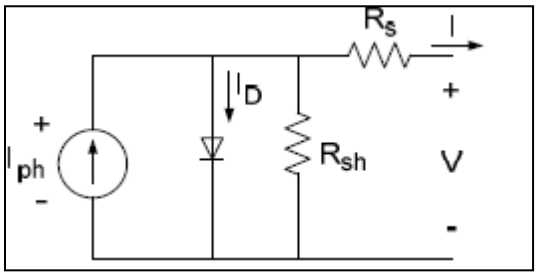

Fig. 3 Equivalent circuit of a solar cell.

C. Modeling of PV Panel

Fig. 3 shows the equivalent circuit of a PV panel with a load. The current output of the PV panel is modeled by the following three equations (M. E. Ropp *et al*, 2009; K. H. Chao *et al*, 2008). All the parameters are shown in Table I:

$$I_{pv} = n_p I_{ph} - n_p I_{sat} \times \left[exp\left(\left(\frac{q}{AKT} \right) \left(\frac{V_{pv}}{n_s} + I_{pv} R_s \right) \right) - 1 \right] \quad (1)$$

$$I_{ph} = \left(I_{sso} + k_i (T - T_r) \right) . \frac{S}{1000} \quad (2)$$

$$I_{sat} = I_{rr} \left(\frac{T}{T_r} \right)^3 exp\left(\left(\frac{qE_{gap}}{kA} \right) . \left(\frac{1}{T_r} - \frac{1}{T} \right) \right) \quad (3)$$

D. Modeling of Battery

Two important parameters to represent state of a battery are terminal voltage V_b and state of charge (SOC) as follows (O. Tremblay *et al*, 2007)

$$V_b = V_0 + R_b . i_b - K \frac{Q}{Q + \int i_b dt} + A . exp(B \int i_b dt) \quad (4)$$

$$SOC = 100 \left(1 + \frac{\int i_b dt}{Q} \right) \quad (5)$$

where R_b is internal resistance of the battery, V_o is the open circuit voltage of the battery, i_b is battery charging current, K is polarization voltage, Q is battery capacity, A is exponential voltage, and B is exponential capacity.

Table 1 Parameters of DFIG

Symbol	Description	Value
P_{nom}	Nominal power	50 *kW*
V_{nom}	Nominal voltage	400 *V*
R_s	Stator resistance	0.00706 *pu*
L_s	Stator inductance	0.171 *pu*
R_r	Rotor resistance	0.005 *pu*
L_r	Rotor inductance	0.156 *pu*
L_m	Mutual inductance	2.9 *pu*
J	Rotor inertial constant	3.1 s
n_p	Number of poles	6
V_{dc_nom}	Nominal DC voltage of AC/DC/AC converter	800 *V*
P_m	Nominal mechanical power	45 *kW*

E. Modeling of Wind Turbine Generator

Power output P_m from a WTG is determined by (6)

$$P_m = 0.5 \rho A C_p (\lambda, \beta) V_w^3 \quad (6)$$

where ρ is air density, A is rotor swept area, V_w is wind speed, and $C(\lambda \beta)$ is the power coefficient, which is the function of tip speed ratio λ and pitch angle β.

The mathematical models of a DFIG are essential requirements for its control system. The voltage equations of an induction motor in a rotating d-q coordinate are as follows:

$$\begin{bmatrix} u_{ds} \\ u_{qs} \\ u_{dr} \\ u_{qr} \end{bmatrix} = \begin{bmatrix} -R_s & 0 & 0 & 0 \\ 0 & -R_s & 0 & 0 \\ 0 & 0 & R_r & 0 \\ 0 & 0 & 0 & R_r \end{bmatrix} \begin{bmatrix} i_{ds} \\ i_{qs} \\ i_{dr} \\ i_{qr} \end{bmatrix} + p \begin{bmatrix} \lambda_{ds} \\ \lambda_{qs} \\ \lambda_{dr} \\ \lambda_{qr} \end{bmatrix} + \begin{bmatrix} -w_1 \lambda_{qs} \\ w_1 \lambda_{ds} \\ -w_2 \lambda_{qr} \\ w_2 \lambda_{dr} \end{bmatrix} \quad (7)$$

$$\begin{bmatrix} \lambda_{ds} \\ \lambda_{qs} \\ \lambda_{dr} \\ \lambda_{qr} \end{bmatrix} = \begin{bmatrix} -L_s & 0 & L_m & 0 \\ 0 & -L_s & 0 & L_m \\ -L_m & 0 & R_r & 0 \\ 0 & -L_m & 0 & L_r \end{bmatrix} \begin{bmatrix} i_{ds} \\ i_{qs} \\ i_{dr} \\ i_{qr} \end{bmatrix} \quad (8)$$

The dynamic equation of the DFIG

$$\frac{J}{n_p} \frac{dw_r}{dt} = T_m - T_{em} \quad (9)$$

$$T_{em} = n_p L_m (i_{qs} i_{dr} - i_{ds} i_{qr}) \quad (10)$$

where the subscripts d, q, s, and r denote d-axis, q-axis, stator, and rotor respectively, L represents the inductance, λ is the flux linkage, u and i represent voltage and current respectively, ω_1 and ω_2 are the angular synchronous speed and slip speed respectively, $\omega_2 = \omega_1 - \omega_r$, T_m is the mechanical torque, T_{em} is the

electromagnetic torque and other parameters of DIFG are listed in Table 1

If the synchronous rotating d-q reference is oriented by the stator voltage vector, the d-axis is aligned with the stator voltage vector while the q-axis is aligned with the stator flux reference frame. Therefore, $\lambda_{ds}=0$ and $\lambda_s=\lambda_s$. The following equations can be obtained in the stator voltage oriented reference frame as (D. W. Zhi *et al*, 2007) :

$$i_{qs}=-\frac{L_m}{L_s}i_{dr},\ T_{em}=n_p\frac{L_m}{L_s}\lambda_s i_{dr}\ \ \sigma=\frac{L_sL_r-L_m^2}{L_sL_r} \tag{11}$$

$$u_{dr}=R_r i_{dr}+\sigma L_r\frac{di_{dr}}{dt}-(w_1-w_r)\left(L_m i_{qs}+L_r i_{qr}\right) \tag{12}$$

$$u_{qr}=R_r i_{qr}+\sigma L_r\frac{di_{qr}}{dt}-(w_1-w_r)(L_m i_{ds}+L_r i_{dr}) \tag{13}$$

3. Coordination Control of the Converters

There are five types of converters in the Micro Grid. Those converters have to be coordinately controlled with the utility grid to supply an uninterrupted, high efficiency, and high quality power to variable DC and AC loads under variable solar irradiation and wind speed when the Micro Grid operates in both isolated and grid tied modes. The control algorithms for those converters are presented in this section.

A. Grid-Connected Mode

When the Micro Grid operates in this mode, the control objective of the boost converter is to track the MPPT of the PV array by regulating its terminal voltage. The back-to-back ac/dc/ac converter of the DFIG is controlled to regulate rotor side cur-rent to achieve MPPT and to synchronize with ac grid. The energy surplus of the Micro Grid can be sent to the utility system. The role of the battery as the energy storage becomes less important because the power is balanced by the utility grid. In this case, the only function of the battery is to eliminate frequent power transfer between the dc and ac link. The dc/dc converter of the battery can be controlled as the energy buffer using the technique (L. Bo *et al*, 2005) . The main converter is designed to operate bi-directionally to incorporate complementary characteristic of wind and solar sources (S. A. Daniel *et al*, 2004; C. Wang *et al*, 2008). The control objectives of the main converter are to maintain a stable dc-link voltage for variable dc load and to synchronize with the ac link and utility system.

The combined time average equivalent circuit model of the booster and main converter is shown in Fig. 4 based on the basic principles and descriptions in (C. Wang *et al*, 2008; M. E. Ropp *et al*, 2009) for booster and in-verter respectively.

Power flow equations at the dc and ac links are as follows:

$$P_{pv}+P_{ac}=P_{dcL}+P_v \tag{14}$$

$$P_s=P_w-P_{acL}-P_{ac} \tag{15}$$

where real power P_v and P_w are produced by PV and WTG respectively, P_{acL} and P_{dcL} are real power loads connected to ac and dc buses respectively, P_{ac} is the power exchange between ac and dc links, P_b is power injection to battery, and P_s is power injection from the Micro Grid grid to the utility.

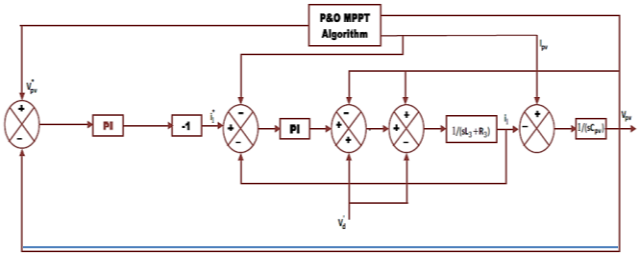

Fig. 4 Time average model for the booster and main converter.

The current and voltage equations at dc bus are as follows:

$$V_{pv}-V_T=L_1\frac{di_1}{dt}+R_1 i_1 \tag{16}$$

$$I_{pv}-i_1=C_{pv}.\frac{dV_{pv}}{dt} \tag{17}$$

$$V_T=V_d.(1-d_1) \tag{18}$$

$$i_1(1-d_1)=C_d\frac{dV_d}{dt}-\frac{1}{R_L}V_d-i_b-i_{ac}=0 \tag{19}$$

where d_1 is the duty ratio of switch ST.

Equations (20) and (21) show the ac side voltage equations of the main converter in ABC and d-q coordinates respectively (O. Tremblay *et al*, 2007)

$$L_2\frac{d}{dt}\begin{bmatrix}i_A\\ i_B\\ i_C\end{bmatrix}+L_2\frac{d}{dt}\begin{bmatrix}i_A\\ i_B\\ i_C\end{bmatrix}=\begin{bmatrix}v_{CA}\\ V_{CB}\\ V_{CC}\end{bmatrix}-\begin{bmatrix}v_{SA}\\ V_{SB}\\ V_{SC}\end{bmatrix} \tag{20}$$

$$L_2\frac{d}{dt}\begin{bmatrix}i_d\\ i_q\end{bmatrix}=\begin{bmatrix}-R_2 & wL_2\\ -wL_2 & -R_2\end{bmatrix}\begin{bmatrix}i_d\\ i_q\end{bmatrix}+\begin{bmatrix}v_{cd}\\ v_{cq}\end{bmatrix}-\begin{bmatrix}v_{sd}\\ v_{sq}\end{bmatrix} \tag{21}$$

Where V_{CA}, V_{CB}, V_{CC} are voltages of the main converter. V_{SA}, V_{SB}, V_{SC} are voltages across C_2 as shown in figure 2. Vsd, Vsq, Vcd, Vcq are corresponding cofficients

In order to maintain stable operation of the Micro Grid under various supply and demand conditions, a coordination control algorithm for booster and main converter is proposed based on basic control algorithms of the grid interactive inverter in (M. E. Ropp *et al*, 2009). The control block diagram is shown in Fig. 5.

The reference value of the solar panel terminal voltage V^*V_p is determined by the basic perturbation and observation (P&O) algorithm based on solar irradiation and temperature to harness the maximum power (D. Salomonsson *et al*, 2007; A. Sannino *et al*, 2003). Dual-

loop control for the dc/dc boost converter is described in (M. E. Baran *et al*, 2003), where the control objective is to provide a high quality dc voltage with good dynamic response. This control scheme is applied for the PV system to track optimal solar panel terminal voltage using the MPPT algorithm with minor modifications. The outer voltage loop can guarantee voltage reference tracking with zero steady-state error and the inner current loop can improve dynamic response.

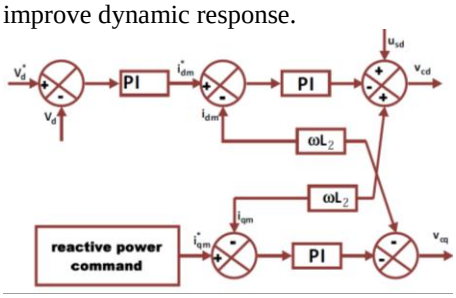

Fig. 5 The control block diagram.

B. Fuzzy Logic Controllers

The word Fuzzy means vagueness. Fuzziness occurs when the boundary of piece of information is not clear-cut. In 1965 Lotfi A. Zahed propounded the fuzzy set theory. Fuzzy set theory exhibits immense potential for effective solving of the uncertainty in the problem. Fuzzy set theory is an excellent mathematical tool to handle the uncertainty arising due to vagueness. Understanding human speech and recognizing handwritten characters are some common instances where fuzziness manifests. Fuzzy set theory is an extension of classical set theory where elements have varying degrees of membership. Fuzzy logic uses the whole interval between 0 and 1 to describe human reasoning. In FLC the input variables are mapped by sets of membership functions and these are called as FUZZY SETS.

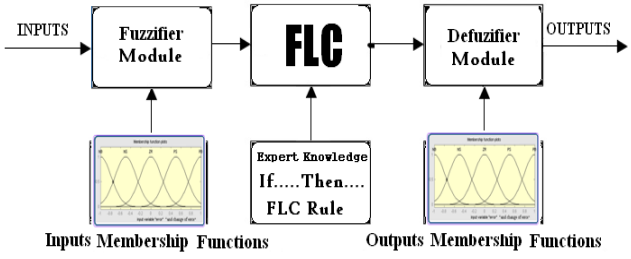

Fig.5.1 Fuzzy Basic Module

Fuzzy set comprises from a membership function which could be defines by parameters. The value between 0 and 1 reveals a degree of membership to the fuzzy set. The process of converting the crisp input to a fuzzy value is called as fuzzificaton. The output of the Fuzzier module is interfaced with the rules. The basic operation of FLC is constructed from fuzzy control rules utilizing the values of fuzzy sets in general for the error and the change of error and control action.

3. Fuzzy Rules

Control strategy based on 49 Fuzzy controls Rule with combination of seven error states multiplying with seven change of error states

Control	Δe	NL	NM	NS	ZR	PS	PM	PL
e								
NL		NL	NL	NL	NL	NL	NL	NL
NM		NL	NL	NM	NM	NS	NS	NS
NS		NL	NM	NM	NS	NS	NS	ZR
ZR		ZR	ZR	ZR	ZR	ZR	ZR	ZR
PS		ZR	PS	PS	PS	PM	PM	PL
PM		PS	PS	PS	PM	PM	PL	PL
PL		PL	PL	PL	PL	PL	PL	PL

Fig 5.2 Control strategy based on 49 Fuzzy controls Rule

4. Simulation Results

The operations of the Micro Grid grid under various source and load conditions are simulated to verify the proposed control algorithms. The parameters of components for the micro grid.

A. Grid-Connected Mode

In this mode, the main converter operates in the PQ mode. Power is balanced by the utility grid. The battery is fully charged and operates in the rest mode in the simulation. AC bus voltage is maintained by the utility grid and dc bus voltage is maintained by the main converter.

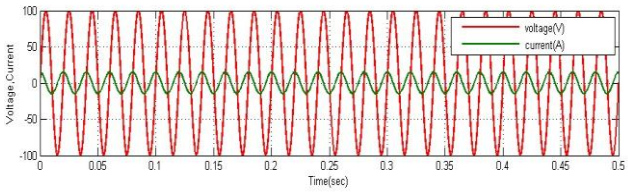

Fig.6 Microgrid voltage and current with Fuzzy Controller.

The optimal terminal voltage is determined using the basic P&O algorithm based on the corresponding solar irradiation. The voltages for different solar irradiations with Micro grid are shown in Fig. 6. The solar irradiation level is set as 400 W/m$_2$ from 0.0 s to 0.1 s, increases linearly to 1000 W/m$_2$ from 0.1 s to 0.2 s, keeps constant until 0.3 s, decreases to 400 W/m$_2$ from 0.3 s to 0.4 s and keeps that value until the final time 0.5 s. The initial voltage for the P&O is set at 250 V. It can be seen that the P&O is continu-ously tracing the optimal voltage from 0 to 0.2 s. The algorithm only finds the optimal voltage at 0.2 s due to the slow tracing speed. The algorithm is searching the new optimal voltage from 0.3 s and finds the optimal voltage at 0.48 s. It can be seen that the basic algorithm can correctly follow the change of solar irradiation but needs some time to search the optimal voltage. The improved P&O methods with fast tracing speed should be used in the PV sites with fast variation of solar irradiation.

Fig. 7 shows the curves of the solar radiation (radiation level times 30 for comparison) and the output power of the PV panel. The output power varies from 13.5 kW to 37.5 kW, which closely follows the solar irradiation when the ambient temperature is fixed.

PV output power versus solar irradiation and AC side voltage and current of the main converter with variable solar irradiation level and constant dc load with Fuzzy Controller.

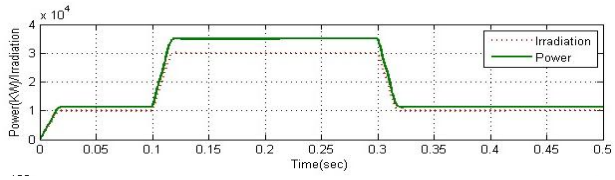

Fig. 7 Curves of the solar radiation

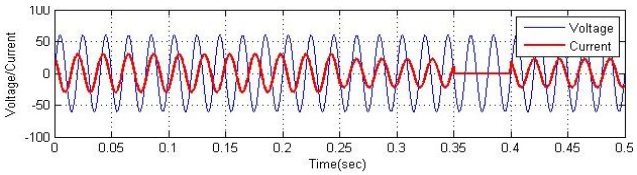

Fig. 8 Voltage and current responses

Fig. 8 shows the voltage (voltage times 0.2 for comparison) and current responses at the ac side of the main converter when the solar irradiation level decreases from 1000 W/m$_2$ at 0.3 s to 400 W/m$_2$ at 0.4 s with a fixed dc load 20 kW. It can be seen from the current directions that the power is injected from the dc to the ac grid before 0.3 s and reversed after 0.4 s.

Lower: AC side voltage versus cur-rent (Voltage times 1/3 for comparison) with Fuzzy Controller.

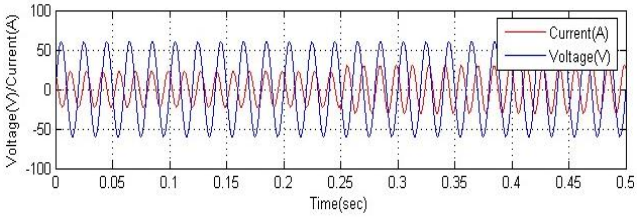

Fig.9 voltage (voltage times 0.2 for comparison) and current responses at the ac side of the main converter when the dc load increases from 20 kW to 40 kW at 0.25 s with a fixed irradiation level 750 W/m$_2$

Fig. 9 shows the voltage (voltage times 0.2 for comparison) and current responses at the ac side of the main converter when the dc load increases from 20 kW to 40 kW at 0.25 s with a fixed irradiation level 750 W/m$_2$. It can be seen from the current direction that power is injected from dc to ac grid before 0.25 s and reversed after 0.25 s. Fig. 15 shows the voltage response at dc side of the main converter under the same conditions. The figure shows that the voltage drops at 0.25 s and recovers quickly by the controller.

B. Isolated Mode

The control strategies for the normal case and Case 1 are verified. In the normal case, Fig.10. DC bus voltage is maintained stable by the battery converter and ac bus voltage is provided by the main converter. The reference of dc-link voltage is set as 400 V. Fig. 11 shows the dynamic responses at the ac side of the main converter when the ac load increases from 20 kW to 40 kW at 0.3 s with a fixed wind speed 12 m/s. It is shown clearly that the ac grid injects power to the dc grid before 0.3 s and receives power from the dc grid after 0.3 s. The voltage at the ac bus is kept 326.5 V constant regardless of load conditions. The nominal voltage and rated capacity of the battery are selected as 200 V and 65 Ah respectively. Fig. 16 also shows the transient process of the DFIG power output, which becomes stable after 0.45 s due to the mechanical inertia.

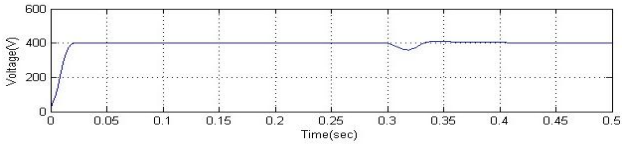

Fig. 10 DC bus voltage transient response with Fuzzy Controller

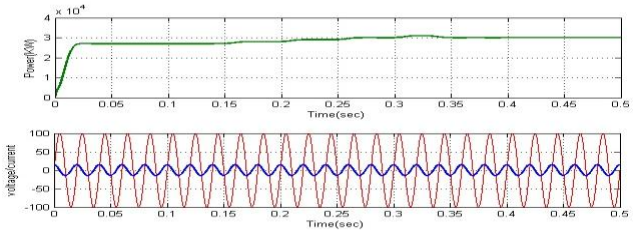

Fig. 11 Upper: output power of the DFIG; Lower: AC side voltage versus cur-rent (Voltage times 1/3 for comparison) with Fuzzy Controller.

The SOC increases and decreases before and after 0.3 s respectively. Fig. 12 shows that the voltage drops at 0.3 s and recovers to 400 V quickly. When the system is at off-MPPT mode in Case 1, the dc bus voltage is maintained stable by the boost converter and ac bus voltage is provided by the main converter. Fig. 13 shows the dc bus voltage, PV output power, and battery charging current respectively when the dc load decreases from 20 kW to 10 kW at 0.2 s with a constant solar irradiation level 1000 W/m$_2$. The battery discharging current is kept constant at

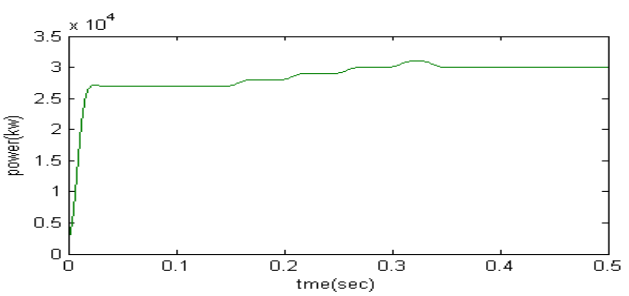

Fig. 12 DC bus voltage transient response in isolated mode with Fuzzy Controller.

65 A. The dc bus voltage is stabilized to 400 V after 0.05 s from the load change. The PV power output drops from the maximum value after 0.2 s, which means that the operating modes are changed from MPPT to off-MPPT mode. The PV output power changes from 35 kW to 25 kW after 0.2 s.

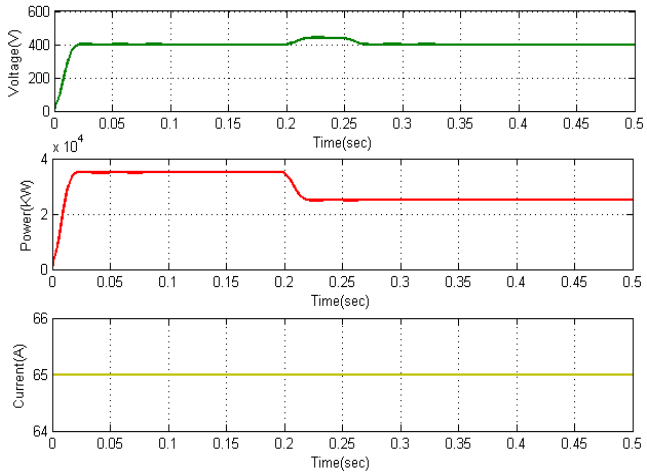

Fig. 13 DC bus voltage, PV output power, and battery current for Case 1 with Fuzzy Controller.

5. Conclusion

A micro grid is proposed Analyses of models and coordination control schemes are proposed for the all the converters to maintain stable system operation under various load and resource conditions. The coordinated control strategies are verified by Matlab/Simulink. Various control methods have been incorporated to harness the maximum power from dc and ac sources and to coordinate the power exchange between dc and ac grid. Different resource conditions and load capacities are tested to validate the control methods. The simulation results show that the Micro Grid can operate stably in the grid-tied or isolated mode. Stable ac and dc bus voltage can be guaranteed when the operating conditions or load capacities change in the two modes. In the paper load demand is met from the combination of PV array, wind turbine and the battery. An inverter is used to convert output from solar & DFIG wind systems into AC power output. Circuit Breaker is used to connect an additional load is given in time. This Micro Grid system is controlled to give maximum output power under all operating conditions to meet the load. Either wind or solar system is supported by the battery to meet the load. Also, simultaneous operation of wind and solar system is supported by battery for the same load.

6. Future scope

1) The losses incurred at the initial working stage of DFIG wind turbine can be controlled through optimum modeling of essential parameters.
2) Dump Load can be used to dispose excess power
3) Transformer can be added to distribute supply variedly to the load
4) PID/FUZZY/ANN controllers can be used to control current in required circuit.
5) Other methods of MPPT can be implemented and compared
6) A current controller is designed to react to and absorb unanticipated Power disturbances in the utility grid

References

R. H. Lasseter, (2002), MicroGrids, in *Proc. IEEE Power Eng. Soc. Winter Meet.*, vol. 1, pp. 305–308.

Y. Zoka, H. Sasaki, N. Yorino, K. Kawahara, and C. C. Liu, (2004),An inter-action problem of distributed generators installed in a MicroGrid, in *Proc. IEEE Elect. Utility Deregulation, Restructuring. Power Technol.*, vol. 2, pp. 795–799.

R. H. Lasseter and P. Paigi, (2004), Microgrid: A conceptual solution, in *Proc. IEEE 35th PESC*, vol. 6, pp. 4285–4290.

C. K. Sao and P. W. Lehn, (2008), Control and power management of con-verter fed MicroGrids, *IEEE Trans. Power Syst.*, vol. 23, no. 3, pp. 1088–1098.

T. Logenthiran, D. Srinivasan, and D. Wong, (2008), Multi-agent coordination for DER in MicroGrid, in *Proc. IEEE Int. Conf. Sustainable Energy Technol*, pp. 77–82.

M. E. Baran and N. R. Mahajan, (2003), DC distribution for industrial sys-tems: Opportunities and challenges, *IEEE Trans. Ind. Appl.*, vol. 39, no. 6, pp. 1596–1601.

Y. Ito, Z. Yang, and H. Akagi, (2004), DC micro-grid based distribution power generation system, in *Proc. IEEE Int. Power Electron. Motion Control Conf*, vol. 3, pp. 1740–1745.

A. Sannino, G. Postiglione, and M. H. J. Bollen, (2003), Feasibility of a DC network for commercial facilities, *IEEE Trans. Ind. Appl.*, vol. 39, no. 5, pp. 1409–1507.

D. J. Hammerstrom, (2007), AC versus DC distribution systems-did we get it right?, in *Proc. IEEE Power Eng. Soc. Gen. Meet*, pp. 1–5.

D. Salomonsson and A. Sannino, (2007), Low-voltage DC distribution system for commercial power systems with sensitive electronic loads, *IEEE Trans. Power Del.*, vol. 22, no. 3, pp. 1620–1627.

M. E. Ropp and S. Gonzalez, (2009), Development of a MATLAB/simulink model of a single-phase grid-connected photovoltaic system, *IEEE Trans. Energy Conv.*, vol. 24, no. 1, pp. 195–202.

K. H. Chao, C. J. Li, and S. H. Ho, (2008), Modeling and fault simulation of photovoltaic generation systems using circuit-based model, in *Proc. IEEE Int. Conf. Sustainable Energy Technol*, pp. 290–294.

O. Tremblay, L. A. Dessaint, and A. I. Dekkiche, (2007), A generic battery model for the dynamic simulation of Micro Grid electric vehicles, in *Proc. IEEE Veh. Power Propulsion Conf*, pp. 284–289.

D. W. Zhi and L. Xu, (2007), Direct power control of DFIG with constant switching frequency and improved transient performance, *IEEE Trans. Energy Conv.*, vol. 22, no. 1, pp. 110–118.

L. Bo and M. Shahidehpour, (2005), Short-term scheduling of battery in a grid-connected PV/battery system, *IEEE Trans. Power Syst.*, vol. 20, no. 2, pp. 1053–1061.

S. A. Daniel and N. AmmasaiGounden, (2004), A novel Micro Grid isolated gener-ating system based on PV fed inverter-assisted wind-driven induction generators, *IEEE Trans. Energy Conv.*, vol. 19, no. 2, pp. 416–422.

C. Wang and M. H. Nehrir,(2008), Power management of a stand-alone wind/ photovoltaic/fuel cell energy system, *IEEE Trans. Energy Conv.*, vol. 23, no. 3, pp. 957–967.